Stem Cell Research 38 (2019) 101467

Contents lists available at ScienceDirect

Stem Cell Research

journal homepage: www.elsevier.com/locate/scr

Generation of induced pluripotent stem cells-derived hepatocyte-like cells for *ex vivo* gene therapy of primary hyperoxaluria type 1

Julie Estève[a,1], Jean-Marc Blouin[a,1], Magalie Lalanne[a], Lamia Azzi-Martin[b], Pierre Dubus[b], Audrey Bidet[c], Jérôme Harambat[d], Brigitte Llanas[d], Isabelle Moranvillier[a], Aurélie Bedel[a], François Moreau-Gaudry[a], Emmanuel Richard[a,*]

[a] Univ.Bordeaux, INSERM, BMGIC, U1035, CHU Bordeaux, 33076 Bordeaux, France
[b] Univ.Bordeaux, INSERM, BARITON, U1053, CHU Bordeaux, 33076, France
[c] Laboratoire d'hématologie, CHU Bordeaux, Bordeaux, France
[d] Service de Néphrologie pédiatrique, Centre de Référence Maladies Rénales Rares du Sud-Ouest, CHU Bordeaux, 33000 Bordeaux, France

ARTICLE INFO

Keywords:
Hyperoxaluria
Induced pluripotent stem cell
Gene therapy
Hepatic differentiation
Lentiviral vector

ABSTRACT

Primary hyperoxaluria type 1 (PH1) is a rare autosomal recessive disorder of the liver metabolism due to functional deficiency of the peroxisomal enzyme alanine:glyoxylate aminotransferase (AGT). AGT deficiency results in overproduction of oxalate which complexes with calcium to form insoluble calcium-oxalate salts in urinary tracts, ultimately leading to end-stage renal disease. Currently, the only curative treatment for PH1 is combined liver-kidney transplantation, which is limited by donor organ shortage and lifelong requirement for immunosuppression. Transplantation of genetically modified autologous hepatocytes is an attractive therapeutic option for PH1. However, the use of fresh primary hepatocytes suffers from limitations such as organ availability, insufficient cell proliferation, loss of function, and the risk of immune rejection. We developed patient-specific induced pluripotent stem cells (PH1-iPSCs) free of reprogramming factors as a source of renewable and genetically defined autologous PH1-hepatocytes. We then investigated additive gene therapy using a lentiviral vector encoding wild-type AGT under the control of the liver-specific transthyretin promoter. Genetically modified PH1-iPSCs successfully provided hepatocyte-like cells (HLCs) that exhibited significant AGT expression at both RNA and protein levels after liver-specific differentiation process. These results pave the way for cell-based therapy of PH1 by transplantation of genetically modified autologous HLCs derived from patient-specific iPSCs.

1. Introduction

Primary hyperoxalurias (PHs) are rare inborn errors of glyoxylate metabolism characterized by increased synthesis and excretion of the end-product oxalate, and deposition of insoluble calcium oxalate in the kidney and urinary tract (Harambat et al., 2011; Hoppe et al., 2009). Primary hyperoxaluria type 1 (PH1, MIM 259900) is a rare autosomal recessive metabolic disorder occurring in 1 per 120,000 live births. It is caused by a functional deficiency of the liver-specific enzyme alanine:glyoxylate aminotransferase (AGT, EC 2.6.1.44) encoded by the *AGXT* gene (locus 2q37.3), which normally localizes to hepatocyte peroxisome (Santana et al., 2003). AGT uses pyridoxal 5′-phosphate (PLP) as a cofactor and catalyzes the nearly irreversible transfer of the amino group from alanine to glyoxylate to yield pyruvate and glycine. In PH1 patients, glyoxylate cannot be efficiently converted into glycine and is instead oxidized to oxalate by lactate dehydrogenase, leading to hyperoxaluria. Oxalate complexes with calcium in the urinary tract, leading to the formation of insoluble calcium-oxalate salts. The salts readily precipitate in tissues, resulting in kidney stones, kidney damage/failure and injury to other organs, which accounts for all the

Abbrevations: Primary hyperoxaluria type 1, (PH1); alanine:glyoxylate aminotransferase, (AGT); patient-specific induced pluripotent stem cells, (PH1-iPSCs); hepatocyte-like cells, (HLCs); pyridoxal 5′-phosphate, (PLP); lentiviral vectors, (LVs); Sendai virus, (SeV); mouse embryonic fibroblasts, (MEFs); KnockOut™ Serum Replacement, (KOSR); human serum albumin, (HSA); hematoxylin and eosin, (HE); Cytochrome P450 3A4, (CYP3A4); bovine serum albumin, (BSA); transthyretin promoter, (TTRp)

* Corresponding author at: Université de Bordeaux, INSERM U1035, 146 rue Léo Saignat, Bordeaux 33076, France.
E-mail address: emmanuel.richard@u-bordeaux.fr (E. Richard).

[1] Contributed equally.

https://doi.org/10.1016/j.scr.2019.101467
Received 2 October 2018; Received in revised form 30 March 2019; Accepted 19 May 2019
Available online 21 May 2019

pathological characteristics of PH1 including urolithiasis, nephrocalcinosis and systemic oxalosis (Hoppe et al., 2009).

Therapeutic strategies aiming at either reducing oxalate production or degrading excessive oxalate in the body would be beneficial for PH1 patients. In some patients, the disease process can be slowed by implementation of hyper diuresis, low oxalate diet or supplementation with vitamin B6, a precursor of pyridoxal phosphate (Cochat et al., 2012). However, the only curative treatment for PH1 is combined liver-kidney transplantation, which represents a form of enzyme replacement therapy by restoring a normal hepatic AGT activity (Bergstralh et al., 2010; Cochat et al., 2010). Nevertheless, this treatment is limited by organ suitability, significant morbidity and mortality and the lifelong requirement for immunosuppressive agents (Alonso and Ryckman, 1998; Newstead, 1998). Allogeneic hepatocyte transplantation has been investigated as an alternative strategy (Beck et al., 2012; Jiang et al., 2008) but it is unlikely to be successful because the high number of engrafted hepatocytes required for clinical recovery of PH1 can hardly be provided by this procedure. In addition, allogeneic hepatocyte transplantation would still involve lifelong immunosuppression.

Given the limitations of current therapy and the severity of the disease, PH1 is an attractive target for gene therapy, providing both a long-lasting and less costly method for AGT delivery to the liver. *In vivo* gene therapy experiments using either adenoviral vectors (Castello et al., 2016; Salido et al., 2006) or adeno-associated virus vectors (Salido et al., 2011) encoding the human AGT yielded encouraging results in $AGXT^{-/-}$ mice. Nevertheless, long-term correction using non-integrative viral vectors involves iterative injections of vectors, potentially leading to cytotoxicity and immunotoxicity. This pitfall may be overcome by an alternative approach based on *ex vivo* genomic integration of the wild-type human *AGXT* gene into hepatic cells using lentiviral vectors (LVs). LVs are suitable tools for gene therapy by virtue of their ability to stably integrate into the target cell genome and the absence of pre-existing humoral and cellular immunity against vector components in most humans. Moreover, the liver cell transduction efficacy of LVs has been demonstrated in numerous studies, notably in the field of hemophilia gene therapy (Annoni et al., 2013; Cantore et al., 2015; Ohmori et al., 2018), while tissue-specific vector expression can be achieved by addition of internal promoters to HIV-1-derived vectors exhibiting partially deleted LTR sequences (Moreau-Gaudry et al., 2001; Zufferey et al., 1998). Ideally, LVs should target primary human hepatocytes, but the invasiveness of liver biopsies along with the poor growth activity and lifespan of hepatocytes in primary culture limit their use *in vitro* (Fukuda et al., 2017; Laurent et al., 2010). The recent advent of hepatocyte-like cells (HLCs) derived from human induced pluripotent stem cells (iPSCs) (Takahashi et al., 2007) represents an attractive alternative to primary human hepatocytes. Indeed, the capacity of patient-specific iPSCs to differentiate into genetically similar somatic cell types allows the generation of a substantial quantity of patient-specific cells, including hepatocytes, for use as *in vitro* models for disease modeling and toxicological studies, as well as cell or gene therapy (Gao and Liu, 2017; Takayama et al., 2018; Zhang et al., 2011).

In this study, we successfully generated iPSCs derived from a homozygous PH1 patient (PH1-iPSCs) harboring a c.731 T > C mutation (p.I244T) in exon 7 of *AGXT* gene, which is the second most common mutation accounting for PH1 (Santana et al., 2003). Furthermore, we demonstrate for the first time the therapeutic genome modification of HLCs derived from PH1-iPSCs, after transduction with a liver-specific lentiviral vector expressing wild-type AGXT cDNA. These results will contribute to the proof-of-principle of PH1 regenerative medicine, based on the transplantation of autologous HLCs derived from iPSCs.

2. Material and methods

2.1. Cell culture

Cryopreserved primary human fibroblasts were obtained from skin punch biopsies of a healthy volunteer and a PH1-diagnosed patient harboring the homozygous c.731 T > C mutation (p.I244T) in exon 7 of the *AGXT* gene. We obtained written informed consent from both participants. Cells were thawed and cultured for one week on 0.1% gelatin-coated culture plates (Sigma-Aldrich) in complete Dulbecco's Modified Eagle Medium (DMEM) (Life Technologies) containing 10% fetal bovine serum (FBS, Eurobio) and 100 UI/ml penicillin/streptomycin (P/S, Hyclone) before reprogramming. The human hepatoma (HepG2 and Huh7) and human embryonic kidney 293 T (HEK293T) cell lines were maintained in complete DMEM. The human myelogenous K562 cell line was maintained in Roswell Park Memorial Institute medium (RPMI) (Life Technologies), supplemented with 10% FBS and 100 UI/ml P/S.

2.2. Human iPSC culture

Fibroblast-derived iPSCs free of reprogramming transgene were generated by transducing wild-type (WT)- and PH1-fibroblasts with Sendai viral (SeV) particles (Ban et al., 2011) using the CytoTune®-iPS 2.0 Sendai Reprogramming Kit (Invitrogen) according to the manufacturer's instructions. Briefly, fibroblasts were transiently exposed to SeV particles for 20 h at 37 °C and cultured for six additional days in fibroblast culture media. Cells were then transferred onto a feeder layer of mitomycin-inactivated mouse embryonic fibroblasts (MEFs) at multiple densities (850, 1700 and 3400 cells/cm^2) and cultivated in KnockOut DMEM/F12 (Life Technologies) containing 20% KnockOut™ Serum Replacement (KOSR, Life Technologies), 1% non-essential amino acids (Life Technologies), 1% GlutaMAX (Life Technologies), 0.5 mM sodium butyrate (Sigma-Aldrich), 0,1 mM beta-mercaptoethanol (Life Technologies), 50 µg/ml L-Ascorbic acid 2-phosphate sesquimagnesium salt hydrate (Sigma-Aldrich), 10 ng/ml basic fibroblast growth factor (Peprotech) and 100 UI/ml P/S. Four weeks after transduction, emerging iPSC colonies were individually picked up and expanded onto MEF monolayer. Two WT- and two PH1-iPSC clones were further selected on the basis of typical undifferentiated stem cell morphology (high nucleus-to-cytoplasm ratio, defined borders and prominent nucleoli). Selected iPSC clones were finally transferred onto feeder-free Cellartis® DEF-CS™ Culture System (Takara Bio Europe), therefore exhibiting proliferation as monolayer iPSC lines with continuous passaging twice a week, as previously described (Asplund et al., 2016).

2.3. Genomic DNA extraction and amplification

Genomic DNA was isolated using the NucleoSpin® Tissue kit (Macherey-Nagel) according to the manufacturer's instructions and were PCR-amplified using specific primers (online Supplemental Table 1). For fibroblast and iPSC genotyping, PCR products from the *AGXT* exon 7 were analyzed by Sanger sequencing. To assess lentiviral cassette integration into iPSC and HepG2 genome, we designed specific primers to amplify the region overlapping the AGXT or eGFP cDNA sequence and the WPRE sequence (online Supplemental Table 1).

2.4. RNA extraction and RT-PCR analysis

Total RNA was isolated using NucleoSpin® RNA kit (Macherey-Nagel) and cDNA was synthesized using the High-Capacity cDNA Reverse Transcription Kit (Applied Biosystems™) according to the manufacturer's instructions. Cellular expression of pluripotency-associated markers and Sendai reprogramming factors, as well as lentiviral cassette expression, were analyzed by RT-PCR using specific primers (online Supplemental Table 1). We used specific primer sets to

distinguish specifically between endogenous and exogenous *AGXT* expression. Exogenous *AGXT* expression was specifically detected using primer sets located in the 3′ region of the *AGXT* cDNA and the 5′ region of the WPRE sequence (Fig. 4A). Endogenous *AGXT* expression was specifically detected using a forward primer located in exon 10 (coding region) of the endogenous *AGXT* gene and a reverse primer located in exon 11 (3'UTR region) of the endogenous *AGXT* gene. A semi-quantitative real-time PCR (RT-qPCR) assay was used to quantify hepatic markers, endogenous and exogenous *AGXT* expression using the GoTaq® qPCR Master Mix kit (Promega); relative gene expression was normalized to endogenous human ribosomal protein lateral stalk subunit P0 (HuPO) mRNA.

2.5. Alkaline phosphatase activity and immunocytofluorescence

iPSCs were challenged for alkaline phosphatase activity using the Leukocyte Alkaline Phosphatase Kit (Sigma-Aldrich), according to the manufacturer's instructions. For immunocytofluorescence analysis, cells were fixed for 15 min at 4 °C in 4% paraformaldehyde and then washed three times in PBS containing 0,2% Triton X-100 for permeabilization. Cells were blocked in PBS/0,2% Triton X-100/1% human serum albumin (HSA) for 1 h at 4 °C, washed three times with PBS/1% HSA and incubated overnight at 4 °C with primary antibodies diluted at working concentration in PBS/0,2% Triton X-100/1% HSA. After incubation, cells were washed three times with PBS/1% HSA and incubated for 1 h at room temperature with secondary antibodies diluted at working concentration in PBS/0,2% Triton X-100/1% HSA. Cells were washed twice with PBS and finally incubated with 1 × 4,6-diamidino-2-2-phenylindole (DAPI) for 15 min at room temperature. The primary and secondary antibodies used in this study are listed online (Supplemental Table 2). Images were captured with an inverted fluorescence microscope (Nikon Eclipse Ti microscope).

2.6. Teratoma formation and analysis

Teratomas were obtained after injecting 1×10^6 WT- or PH1-iPSCs suspended in extracellular matrix gel (Sigma-Aldrich, St-Louis, MO) in the subcutaneous neck region of immunodeficient NSG mice (NOD Cg-Prkdcscid Il2rgtm1Wjl/SzJ, animal facilities A2, University of Bordeaux, France). Tumors were harvested 6 weeks after injection and fixed in 4% paraformaldehyde. Tissues were paraffin-embedded, sectioned and stained with hematoxylin and eosin (HE), and alcian blue. All animal procedures were approved by the Institutional Animal Care and Use Committee of Bordeaux University.

2.7. Karyotype analysis

WT- and PH1-iPSCs were cultured to 80% confluence in 6-well plates. After synchronization with bromodeoxyuridine, thymidine kinase and colcemid, cells were trypsinized with trypsin/EDTA (0,05%/0,2%) (Fisher Scientific), treated with 0.075 M KCl and prefixed with 1 ml of fixative solution composed of Methanol/Acetic Acid (3:1) and resuspended in 10 ml of fixative solution. Cells were centrifuged for 6 min at 200 *g* before final resuspension in 5 ml of fixative. Standard R-banding analysis was performed on metaphases obtained from iPSC clones. At least 20 metaphases were fully karyotyped with the help of an automated imaging system (MetaSystems).

2.8. Lentiviral vectors and cell transduction

Self-inactivated (SIN) lentiviral vectors derived from the previously described pRRL-MND-MCS-WPRE lentivector (Richard et al., 2004). Lentiviral vectors harbored the optimized human AGXT cDNA (Mesa-Torres et al., 2014) or eGFP cDNA under control of the murine transthyretin promoter (TTRp) fused to a synthetic hepatocyte-specific enhancer to direct liver-specific expression (Nguyen et al., 2005). The modified retroviral MND promoter was used to drive ubiquitous expression of *AGXT* and *eGFP* transgenes (Richard et al., 2004). VSV-G-pseudotyped recombinant lentiviral particles were produced by triple-transient transfection of three plasmids in 293 T cells: the transfer vector plasmid, the packaging plasmid pCMVΔR8.91, and the VSV-G envelope protein-coding plasmid pMD.G as described (Bedel et al., 2012). Titers of eGFP-expressing vectors were determined after serial dilutions in HepG2 hepatoblastoma cell lines. Titers of AGXT-containing lentivectors were estimated on the basis of p24 antigen levels determined by ELISA assay in the viral supernatant (Innotest HIV p24, INGEN SA, Rungis, France), by comparison with that of simultaneously produced eGFP vectors as previously described (Richard et al., 2004). Lentiviral vector supernatants were tested for the absence of replication-competent virus. To evaluate tissue-specific expression of lentiviral vectors, hepatic (Huh7, HepG2), epithelial (HEK293T) and myelogenous (K562) human cell lines, as well as primary human fibroblasts and WT-iPSCs, were transduced with lentiviral vectors at a low multiplicity of infection (m.o.i. = 1) to obtain proviral integration of around one copy/cell. In additive gene therapy experiments, iPSCs from the PH1 patient were transduced at a multiplicity of infection of 5.

2.9. Flow cytometry analysis

At day 7 post-lentiviral transduction, eGFP fluorescence was analyzed using FACSCanto™ II (BD Biosciences) and FACSDiva™ software (BD Biosciences).

2.10. In vitro differentiation of iPSCs toward hepatic lineage

Feeder-free cultured iPSCs were differentiated into hepatocyte-like cells (HLCs) by applying a serum- and feeder-free procedure recapitulating liver development, as previously described (Asplund et al., 2016; Ghosheh et al., 2016). First, iPSCs were guided to differentiate into definitive endoderm cells (DECs) using the Cellartis® Definitive Endoderm Differentiation Kit (Takara Bio Europe), according to the manufacturer's instructions. At day 7, the DECs were enzymatically dissociated with TrypLE™ Select Enzyme (Life Technologies), reseeded into appropriate cell culture vessels, and differentiated into HLCs using the Cellartis® Hepatocyte Differentiation Kit (Takara Bio Europe), according to the manufacturer's instructions.

2.11. Assay for cytochrome P450 activity

Cytochrome P450 3A4 (CYP3A4) activity was measured in iPSCs and HLCs by using the P450-Glo™ CYP3A4 Assay kit (Promega) according to the manufacturer's instructions. Briefly, cells were incubated for 1 h at 37 °C with respective cell culture media containing 3 μM of the CYP3A4 substrate luciferin isopropyl acetal (proluciferin). After incubation, 25 μl of culture media were transferred from each well to a 96-well opaque white luminometer plate. Next, a luciferin detection reagent (25 μl) was added to the samples to initiate a luminescent reaction. The plate was incubated at room temperature for 20 min, and luminescence was measured using a GloMax® Multi Detection System luminometer (Promega). Luminescence signal was standardized for each well by cell protein content determined by the Pierce™ BCA Protein Assay Kit (ThermoScientific), according to the manufacturer's instructions.

2.12. Western blot

Total cellular protein extraction was carried out using T3EN buffer (10 mM Tris base, 150 mM NaCl, 3 mM EDTA, H_2O) and SB2X buffer (4% SDS, 20% glycerol, 50 mM Tris-HCl pH 6.8, H_2O), followed by 10 min incubation at 100 °C. Protein concentration was determined with the Pierce™ BCA Protein Assay Kit (ThermoScientific), according to the manufacturer's instructions. Respectively 20 μg and 1 μg of

protein from HLC and HepG2 lines were separated by electrophoresis on 12% (*w/v*) acrylamide SDS-PAGE and transferred onto a polyvinylidene difluoride Immobilon-P membrane (Millipore Corp.). The blot was blocked with TBS (20 mM Tris-HCl pH 7.6, 136 mM NaCl) containing 5% skimmed milk, and then incubated at 4 °C overnight with primary antibodies diluted at working concentration in TBS containing 5% bovine serum albumin (BSA, Sigma-Aldrich). The following day, the membrane was washed three times for 5 min in TBS with 0.1% Tween 20 (TBS-T) and then incubated with horseradish peroxidase-linked secondary antibodies diluted at working concentration in TBS-milk for 1 h at room temperature. The membrane was washed a further three times for 5 min with TBS-T before developing using the Amersham ECL Prime Western Blotting Detection Reagent kit (GE Healthcare), according to the manufacturer's instructions. Images were captured with the LAS-3000 Imager (Fujifilm). Relative expression was determined by density measurement and standardized as the ratio AGT signal /GAPDH signal using ImageJ software. The primary and secondary antibodies used for western blotting are listed in online Supplemental Table 3.

2.13. AGT enzymatic assay

The AGT enzymatic activity was determined by incubating 500 to 1000 µg of soluble lysate with L-alanine (50 mM) and glyoxylate (50 mM) for 2 h in the presence of pyridoxal-phosphate (50 µM) in 100 mM potassium phosphate buffer, pH 7.4. The reaction was stopped with perchloric acid 1 M and neutralized with morpholinopropanesulphonic acid (Mops 0.2 M). Pyruvate formation was measured by the spectrophotometric assay after incubation with lactate deshydrogenase (LDH) and NADH (0.22 mM) in Tris-Cl 0.37 M pH 8.3 solution.

2.14. Statistical analysis

Values shown represent the mean ± SD ($n = 3$ to 4 independent experiments). *P*-values were determined using a one-way analysis of variance (ANOVA) complemented by Tukey's multiple comparisons test to examine significance across comparisons. Difference was considered significant at $p < 0.05$.

3. Results

3.1. Generation and characterization of iPSCs from PH1 patient-derived dermal cells

Skin fibroblasts were isolated from a healthy volunteer and a PH1-diagnosed patient harboring the homozygous c.731 T > C mutation (p.I244T) in exon 7 of *AGXT* gene (Fig. 1A). WT- and PH1-iPSC lines were generated *in vitro* from primary fibroblasts after transduction with a modified, non-transmissible form of Sendai Virus (SeV) particles carrying the reprogramming factors SOX2, OCT3/4, c-MYC and KLF4, which is sufficient for efficient reprogramming (Takahashi et al., 2007). The exclusive cytoplasmic expression of SeV particles allows the generation of iPSCs free of reprogramming transgenes, as confirmed by RT-PCR analysis. SeV structural genome and exogenous reprogramming transgene expression was detected exclusively in transduced primary fibroblasts (Sendai fibroblasts), whereas non-transduced fibroblasts and iPSC lines (at 18–19 passages) harbored neither SeV genome nor reprogramming transcript expression (Fig. 2A).

iPSCs were established and expanded as individual colonies onto MEFs for 12 weeks. Two isolated WT-iPSC clones (hereinafter named WT-iPSC#1 and WT-iPSC#2) and two isolated PH1-iPSC clones (hereinafter named PH1-iPSC#1 and PH1-iPSC#2) were switched to feeder-free culture conditions using the Cellartis® DEF-CS™ Culture System, which allows enzymatic passaging of pluripotent stem cells and expansion as monolayer iPSC lines. We confirmed the stability of the *AGXT* genotype in all established iPSC lines (Fig. 1B, WT-iPSC#2 and PH1-iPSC#2 and online Supplemental Fig. S1, WT-iPSC#1 and PH1-iPSC#1).

Feeder-free WT and PH1-iPSC lines exhibited undifferentiated stem cell morphology with a high nucleus/cytoplasm ratio and prominent nucleoli (Fig. 2B, WT-iPSC#2 and PH1-iPSC#2 and online Supplemental Fig. S2, WT-iPSC#1 and PH1-iPSC#1). Moreover, all iPSC clones expressed endogenous pluripotency-associated markers (OCT3/4, SOX2, NANOG, REX1, ESG1, DPPA4, hTERT, KLF4, c-MYC), as demonstrated by alkaline phosphatase activity, immunocytofluorescence (Fig. 2B, WT-iPSC#2 and PH1-iPSC#2 and online Supplemental Fig. S2, WT-iPSC#1 and PH1-iPSC#1) and RT-PCR analysis (Fig. 2C). We detected endogenous expression of *KLF4* and *c-MYC* genes by RT-PCR analysis in primary fibroblasts as previously described (Takahashi et al., 2007). We then generated teratoma by subcutaneous injection of 1×10^6 cells from all WT- and PH1-iPSC lines into 2-month-old immunodeficient NSG mice. About 6 weeks after injection, tumors exhibited goblet cells (endoderm), chondrocytes (mesoderm) and neuroectoderm and pigmented tissue (ectoderm), which demonstrates the ability of iPSCs to differentiate into all three germ layers (Fig. 3A). Finally, karyotype analyses by R-banding studies confirmed the absence of macroscopic genetic abnormality in WT- and PH1-iPSC lines (Fig. 3B, WT-iPSC#2 and PH1-iPSC#2 and online Supplemental Fig. S3, WT-iPSC#1 and PH1-iPSC#1). Therefore, we have successfully committed

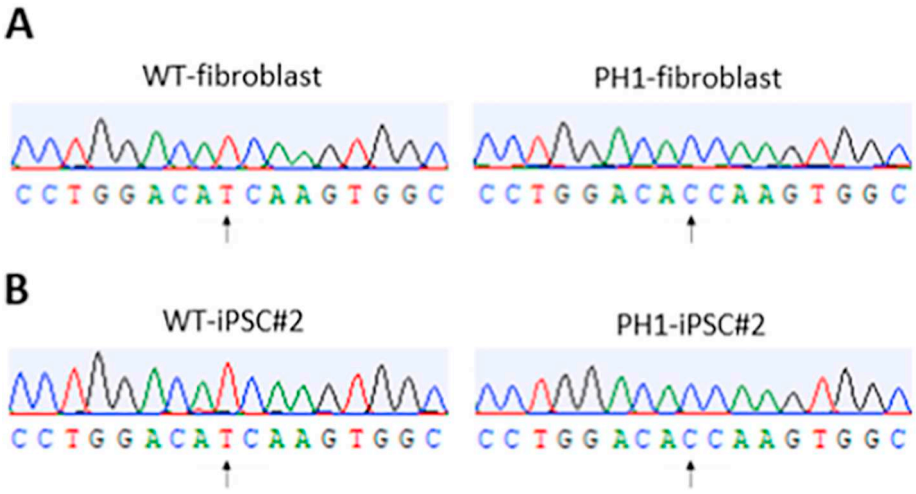

Fig. 1. Analysis of *AGXT* mutations in primary fibroblasts and iPSCs.
The homozygous c.731 T > C *AGXT* mutation was detected in PH1-fibroblasts (A) and PH1-iPSC lines (B) by Sanger sequencing of *AGXT* exon 7.

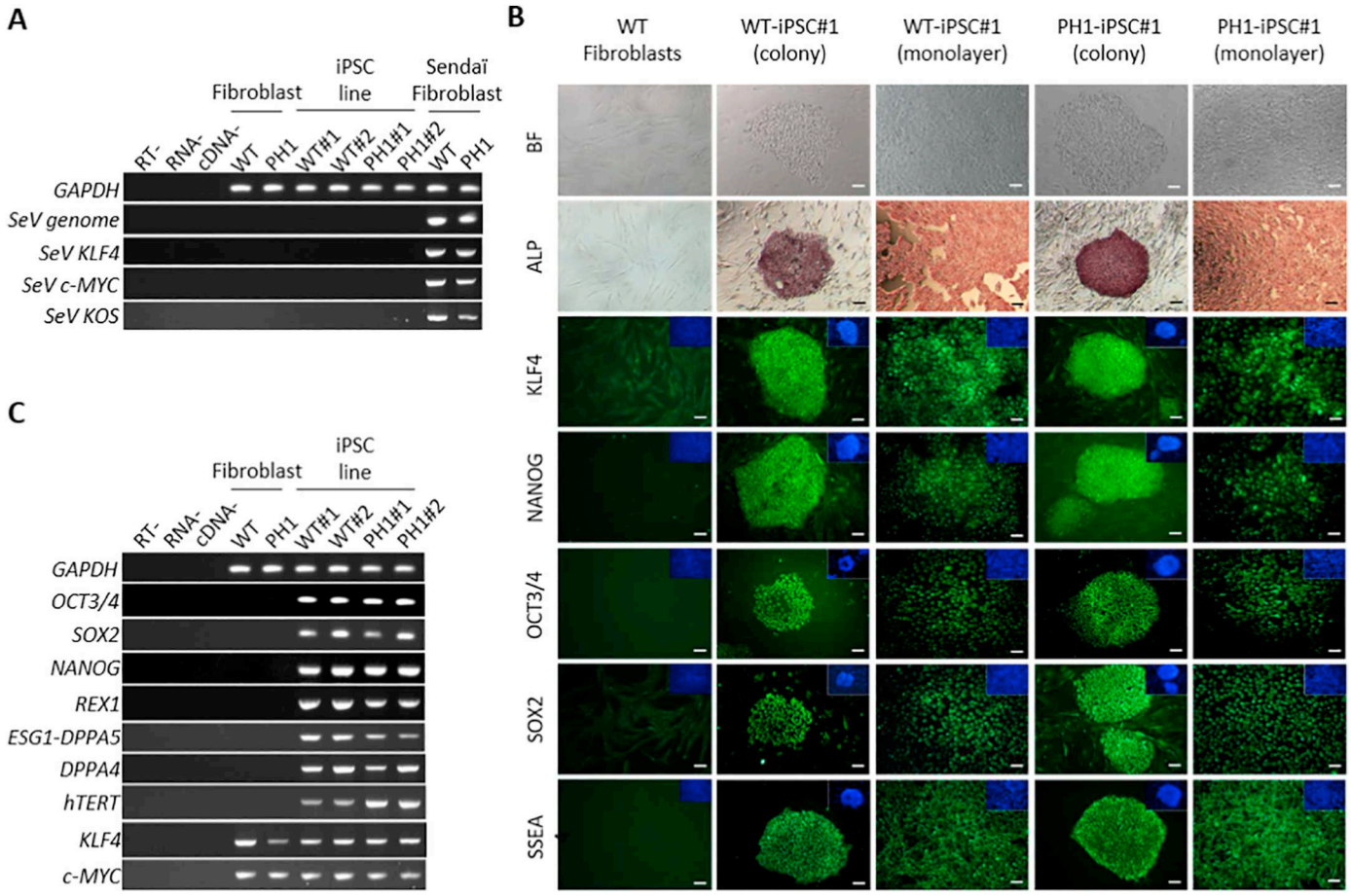

Fig. 2. Generation and characterization of human WT and PH1-iPSCs.
(A) RT-PCR analysis of Sendai virus (SeV) reprogramming factor expression before SeV transduction (Fibroblast), 5 days after SeV transduction (Sendai fibroblast) and in established iPSCs (iPSC line). (B) Analysis of iPSC morphology (BF, bright field), alkaline phosphatase activity (ALP) and pluripotency-associated marker expression (green immunofluorescence staining) in iPSCs expanded on stromal MEF cells (colony) or in feeder-free conditions (monolayer). DAPI staining revealed nuclei (blue). Scale bars, 100 µm. Magnification, 100X. (C) RT-PCR analysis of endogenous pluripotency-associated marker expression in iPSC lines as compared with primary fibroblasts. (For interpretation of the references to colour in this figure legend, the reader is referred to the web version of this article.)

WT- and PH1-fibroblasts in pluripotent stem cells free of reprogramming transgenes that display human embryonic stem cell-like features.

3.2. Lentiviral-mediated delivery of therapeutic AGT in PH1-iPSCs

To trigger wild-type AGT expression in the PH1-iPSC line, we designed a third-generation lentiviral vector (LV) carrying a full-length codon-optimized human AGXT cDNA. Lentiviral constructs carried the modified retroviral MND promoter or the liver-specific transthyretin promoter (TTRp) to drive ubiquitous or liver-specific expression of the therapeutic (*AGXT*) or control (*eGFP*) transgenes, respectively (Fig. 4A). We confirmed ubiquitous and specific expression toward the hepatic lineage after lentiviral transduction of both hepatic (HepG2 and Huh7) and non-hepatic (HEK293T, K562, WT-fibroblast and WT-iPSC#2) cell lines at low multiplicity of infection (m.o.*i* = 1) (Fig. 4B). As expected, MNDp-eGFP lentivector was expressed in each of the different cell lines, while TTRp-eGFP lentivector was selectively expressed in hepatic cells.

We then investigated lentiviral vector-mediated AGXT and eGFP expression in HepG2 cells transduced with the corresponding lentivectors at m.o.i of 5. Once HepG2 genomic integration of the cassettes had been confirmed (Fig. 4C), we observed significant lentiviral vector-mediated transgene expression in transduced HepG2 cells by RT-PCR (Fig. 4D) and western blotting analysis (Fig. 4E). RT-PCR analysis revealed transcriptional expression of TTRp-AGXT and TTRp-eGFP cassettes limited to transduced HepG2 lines, while the endogenous *AGXT* gene was expressed in all conditions (Fig. 4D). Similarly, western blotting analysis using a primary antibody detecting indistinctly both endogenous and exogenous (derived from TTRp-AGXT cassette) AGT revealed basal expression of endogenous AGT in both non-transduced HepG2 and HepG2-TTRp-eGFP lines, while the HepG2-TTRp-AGXT line exhibited a 5-fold increased global AGT expression *vs* no-transduced HepG2 (Fig. 4E). Finally, we obtained ~5-fold increased AGT enzymatic activity in HepG2-TTRp-AGXT as compared with HepG2 cell lines, demonstrating the functional activity of our therapeutic hepatic-specific lentivector (Fig. 4F). These results confirmed therapeutic AGT expression at both transcript and protein levels in the hepatic HepG2 cell line after transduction with the therapeutic TTRp-AGXT lentiviral vector.

We then performed genome modification of PH1-iPSCs by transduction with TTRp-AGXT or TTRp-eGFP lentivector at m.o.i. of 5. We preferentially targeted PH1-iPSC#2 because we observed sustained proliferation and maintenance of stem-cell morphology characteristics through passages of this clone (data not shown). PCR analysis confirmed genomic integration of lentivectors into transduced iPSC lines, referred to as PH1-iPSC#2-TTRp-AGXT and PH1-iPSC#2-TTRp-eGFP lines, respectively (Fig. 4F).

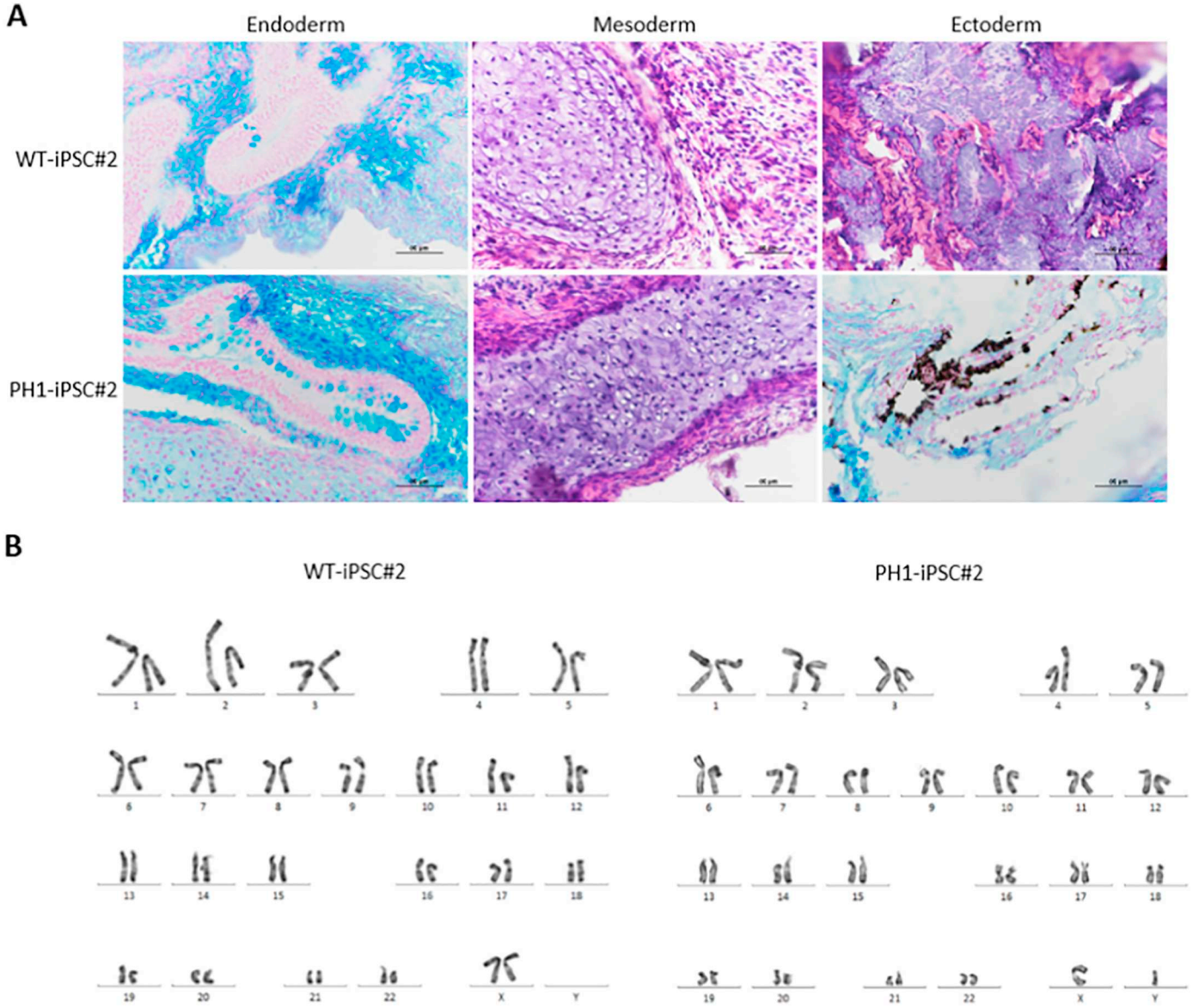

Fig. 3. Teratoma and karyotype analysis.
(A) Alcian blue and hematoxylin/eosin staining of histological sections of a representative teratoma derived from WT-iPSC#2 and PH1-iPSC#2 shows tissues of all three germ layers. Scale bars, 50 µm. Magnification, 40CX. (B) Representative karyotype analysis of WT-iPSC#2 (46, XX) and PH1-iPSC#2 (46, XY) revealed no abnormalities. (For interpretation of the references to colour in this figure legend, the reader is referred to the web version of this article.)

3.3. AGT rescue in iPSC-derived hepatocyte-like cells transduced with TTRp-AGXT lentivector

We next proceeded to *in vitro* differentiation of WT-iPSC#2, PH1-iPSC#2, PH1-iPSC#2-TTRp-AGXT and PH1-iPSC#2-TTRp-eGFP lines into hepatocyte-like cells (HLCs), respectively named WT-HLC#2, PH1-HLC#2, PH1-HLC#2-TTRp-AGXT and PH1-HLC#2-TTRp-eGFP. We used a protocol simulating normal liver development in three main phases: definitive endoderm, hepatic progenitors and hepatocyte-like cells. During the first phase, we used the Cellartis® Definitive Endoderm Differentiation medium to differentiate iPSCs into a monolayer culture of definitive endoderm cells (DECs), which represent the earliest precursors of all endodermal organs; namely, liver, pancreas, lung, gut and thyroid (Hannan et al., 2013). Whereas iPSC lines showed typical embryonic stem cell morphology prior to the differentiation process, they progressively exhibited spiky or triangular shapes, a typical morphology of DEC reaching confluence (Fig. 5A). We confirmed definitive endoderm commitment by immunofluorescence detection of the specific endodermal marker SOX17 at day 7 of differentiation (Fig. 5A).

During the second phase, we guided DECs to subsequent hepatoblast and HLC differentiation for 3 weeks in Cellartis® Hepatocyte Differentiation medium. The cellular morphology progressively changed during the differentiation process to finally reach typical hepatocyte-like polygonal shape with canaliculated borders from day 21 of differentiation (Fig. 5A). Immunofluorescence analysis confirmed hepatic cell commitment, as demonstrated by the specific expression of the hepatic markers HNF4a and alpha-fetoprotein (aFP) in HLC by day 14 and day 21 of differentiation respectively. By day 31, we compared the expression profile of several hepatic markers (albumin, aFP, alpha-1 antitrypsin (a1AT) and HNF4a) between iPSC lines, iPSC-derived hepatocyte-like cells, primary fetal hepatocytes and primary adult hepatocytes (Fig. 5B). Although we observed evidence of liver-specific expression in HLCs generated in our culture system, we acknowledge that these cells were not terminally differentiated, as evidenced by remaining aFP expression. This observation is consistent with previous studies demonstrating that pluripotent stem cell-derived hepatocyte-

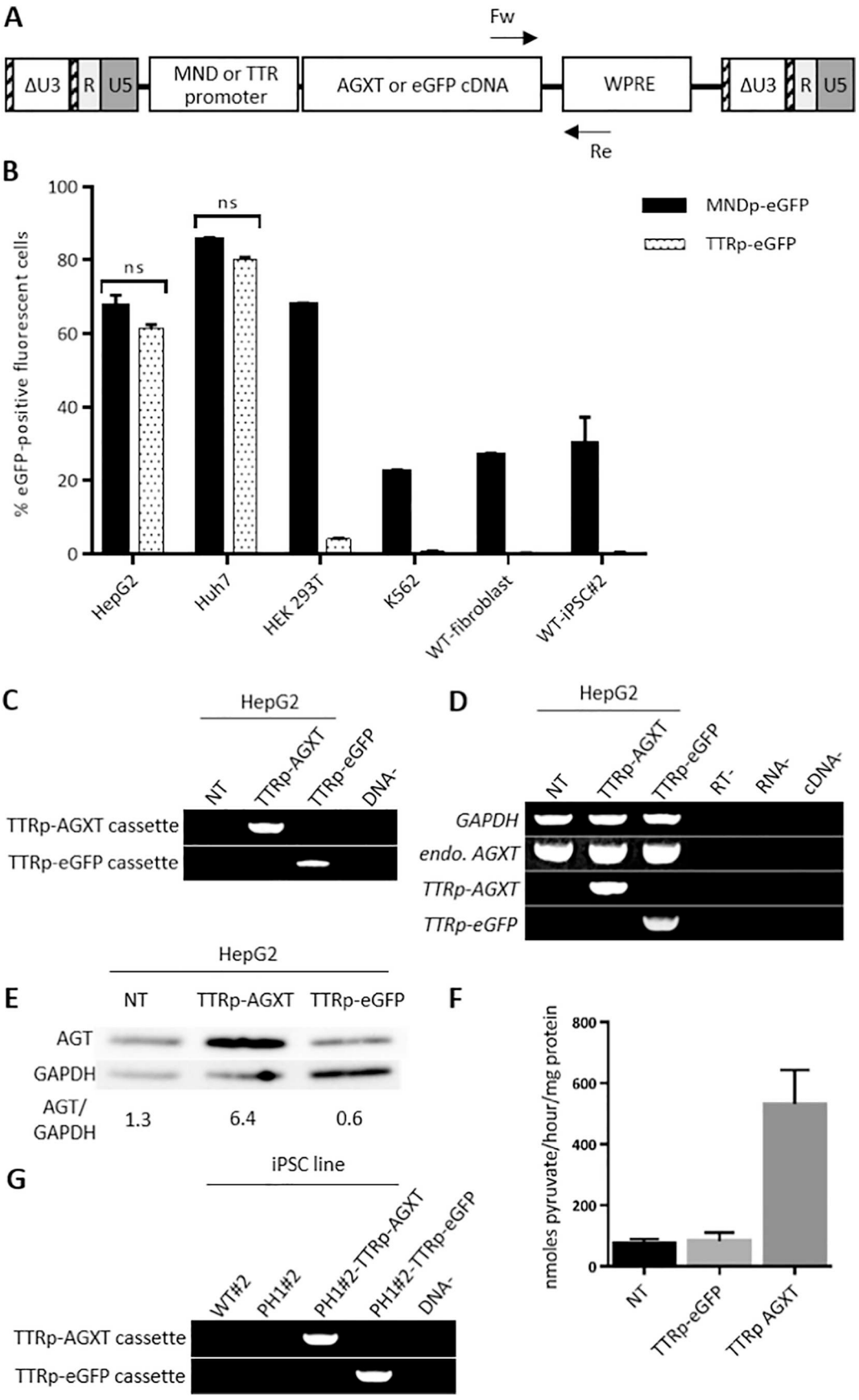

(caption on next page)

Fig. 4. Characterization of the therapeutic AGT-expressing liver-specific lentiviral vector.
(A) Lentiviral vector construct and PCR primer location used for proviral integration analysis. (B) Analysis of eGFP expression in hepatic (HepG2 and Huh7) and non-hepatic (HEK 293T, K562, WT-fibroblast and WT-iPSC#2) cells after lentiviral transduction. eGFP expression was detected by flow cytometry analysis and data were expressed as means ± SD of four independent experiments. (C) PCR analysis of proviral integration in transduced HepG2 cells. (D) RT-PCR analysis of eGFP and AGXT expression in transduced HepG2 cells. (E) Western blotting analysis of AGT protein expression in transduced HepG2 cells. GAPDH was used as control housekeeping gene. (F) PCR analysis of proviral integration in transduced PH1-iPSC#2 cells. Abbreviations: ns, non-significant; endo., endogenous.

like cells more similarly mimic fetal rather than adult hepatocytes (Baxter et al., 2015; Rashid et al., 2010). Detoxification activity of cytochrome P450 3A4 (CYP3A4), which corresponds to the most abundant CYP450 expressed in adult liver (Guengerich, 1999), was also evaluated (Fig. 5C). CYP3A4 activity was significantly higher in HLCs (25- to 40-fold increase) than in undifferentiated control iPSCs. Interestingly, PH1-HLC#2 cell lines showed similar CYP3A4 activity, independently of the genetic modification (TTRp-AGXT, TTRp-eGFP, mock), which suggests homogeneous hepatic differentiation.

We then analyzed the therapeutic benefit of *AGXT* additive gene therapy in PH1-HLCs. We evaluated AGT rescue in PH1-iPSC-derived HLC after transduction with TTRp-AGXT or TTRp-eGFP lentivectors. RT-PCR analysis revealed transcriptional expression of TTRp-AGXT and TTRp-eGFP lentivectors exclusively in PH1-HLC#2-TTRp-AGXT and PH1-HLC#2-TTRp-eGFP respectively, while endogenous *AGXT* gene was expressed in all HLC lines (Fig. 5D). On the other hand, AGT protein was detected only in WT-HLC#2 and PH1-HLC#2-TTRp-AGXT cells, whereas PH1-HLC#2 and PH1-HLC#2-TTRp-eGFP exhibited no endogenous AGT expression (Fig. 5E). These results suggest that the mutant p.I244T AGT is unstable in HLCs and rapidly turns into non-functional aggregates that are subsequently eliminated before reaching hepatocyte peroxisome. Therefore, we hypothesize that WT-HLC#2 exhibited basal endogenous wild-type AGT expression, whereas the AGT protein detected in PH1-HLC#2-TTRp-AGXT was entirely due to the expression of the therapeutic TTRp-AGXT lentivector. Taken together, these results show that we have achieved the first successful rescue of AGT by using liver-specific lentiviral vector in iPSC-derived hepatocyte-like cells from a PH1 patient.

4. Discussion

PH1 is an inherited metabolic disease arising from the liver deficiency of the AGT enzyme that leads to overproduction of oxalate, which forms insoluble calcium salts in the kidney, resulting in nephrocalcinosis and urolithiasis. Combined liver-kidney transplantation is the only curative treatment for PH1 but it suffers from limitations, which provides the impetus to develop innovative therapeutic options such as liver-directed gene therapy. The recent advent of iPSCs has opened up new avenues in the field of regenerative medicine, and the availability of efficient hepatic differentiation procedures has made iPSCs attractive for the treatment of liver diseases such as PH1 (Asplund et al., 2016; Ghosheh et al., 2016; Hannan et al., 2013; Rashid et al., 2010). In this study, we efficiently generated PH1-iPSCs free of reprogramming factors and expanded them under feeder-free conditions. We then successfully differentiated *in vitro* PH1-iPSCs into hepatocyte-like cells, which are suitable for disease modeling and gene therapy experiments. Finally, we rescued AGT expression in PH1-iPSC-derived HLCs after transduction with a self-inactivated liver-specific lentiviral vector expressing an optimized AGT enzyme.

During the past decade, iPSCs have been generated with several integrative and non-integrative methods, the former exploiting viral vectors integrated in the host cell genome and stably expressing the transgene, and the latter including any approach that enables transient transgene expression in target cells. However, the persistence of residual transgene expression may alter the potential for iPSC differentiation or induce malignant transformation (Okita and Yamanaka, 2011). Sendai vectors are the safest and most commonly used viral-based approach to obtain iPSCs using non-integrative methods. Furthermore, they allow the generation of iPSCs with much greater efficiency than the conventional integrative vectors without influencing the gene expression profile of the reprogrammed iPSCs (Trevisan et al., 2017). In our study, we obtained an initial reprogramming efficiency on feeder cells ranging from 0.002% to 0.08% for PH1- and WT-iPSCs respectively, which corresponds to levels previously reported in the literature (Ban et al., 2011).

Traditional biomedical research and preclinical studies frequently rely on animal models that often fail to reproduce important clinical phenotypes. Conventional cell lines are also frequently used but they represent only a small number of cell types or diseases, and are characterized by limited genetic diversity, rapid senescence and potentially confounding immortalizing mutations. In recent years, human pluripotent stem cells have attracted much attention, partly due to their promising potential for modeling human diseases accurately. In this study, we generated PH1-iPSCs from primary fibroblasts harboring the *AGXT* c.731 T > C mutation, which is highly prevalent in Western Europe, North Africa and the Middle East, as it has been reported in around 20% of PH1 patients from these countries (Harambat et al., 2010). To our knowledge, this is the first report of PH1-iPSC-derived hepatocyte-like cells from a PH1 patient. In a previous study, primary fibroblasts from a PH1 patient harboring the homozygous c.731 T > C mutation in exon 7 of the *AGXT* gene were fully reprogrammed into transgene-free iPSCs using the Sendai virus vector, but the potential for hepatic differentiation was not demonstrated (Zapata-Linares et al., 2016). The p.I244T AGT protein is known to be responsive to pharmacological chaperones such as betaine (Santana et al., 2003), and we believe that the combination of additive *AGXT* gene therapy and pharmacological treatments could significantly improve the phenotype of PH1 patients carrying the c.731 T > C mutation.

To facilitate the differentiation process and subsequent analysis of the hepatocyte phenotype, we expanded WT- and PH1-iPSCs under feeder-free conditions. To date, most pathophysiological studies of *AGXT* mutations have been conducted in the stably transformed CHO-GO cell line overexpressing glycolate oxidase (GO) and WT-AGT or pathogenic variants (Dindo et al., 2018). We propose that HLCs derived from PH1-iPSCs would offer new perspectives for the identification of molecular defects associated with AGT mutations in liver cells. In the future, the generation of iPSCs originating from a wide panel of PH1 patients and their differentiation into hepatocytes could play an important role in the exploration of phenotype/genotype correlations and drug susceptibilities.

The present study goes further by demonstrating the stable genome modification of hepatocyte-like cells derived from PH1-iPSCs, which were previously transduced with a liver-specific self-inactivating lentiviral vector expressing wild-type AGXT cDNA. The AGXT sequence was optimized for expression in human cells (Mesa-Torres et al., 2014) and placed under the control of the liver-specific transthyretin promoter, whose efficacy has already been demonstrated *ex vivo* and *in vivo* in liver-disease animal models (Nguyen et al., 2005; Schmitt et al., 2010). Importantly, we rescued AGT synthesis in PH1-HLC#2-TTRp-AGXT following TTRp-AGXT lentiviral transduction, even though we observed a lower AGT expression level than with WT-HLCs. This might be due to the suboptimal expression of the transthyretin promoter and/or incomplete differentiation state of iPSC-derived HLCs, as previously reported (Baxter et al., 2015; Rashid et al., 2010; Roy-Chowdhury et al., 2017). Integration of the therapeutic TTRp-AGXT lentiviral vector into PH1-iPSCs allowed specific expression of AGT at both transcript and

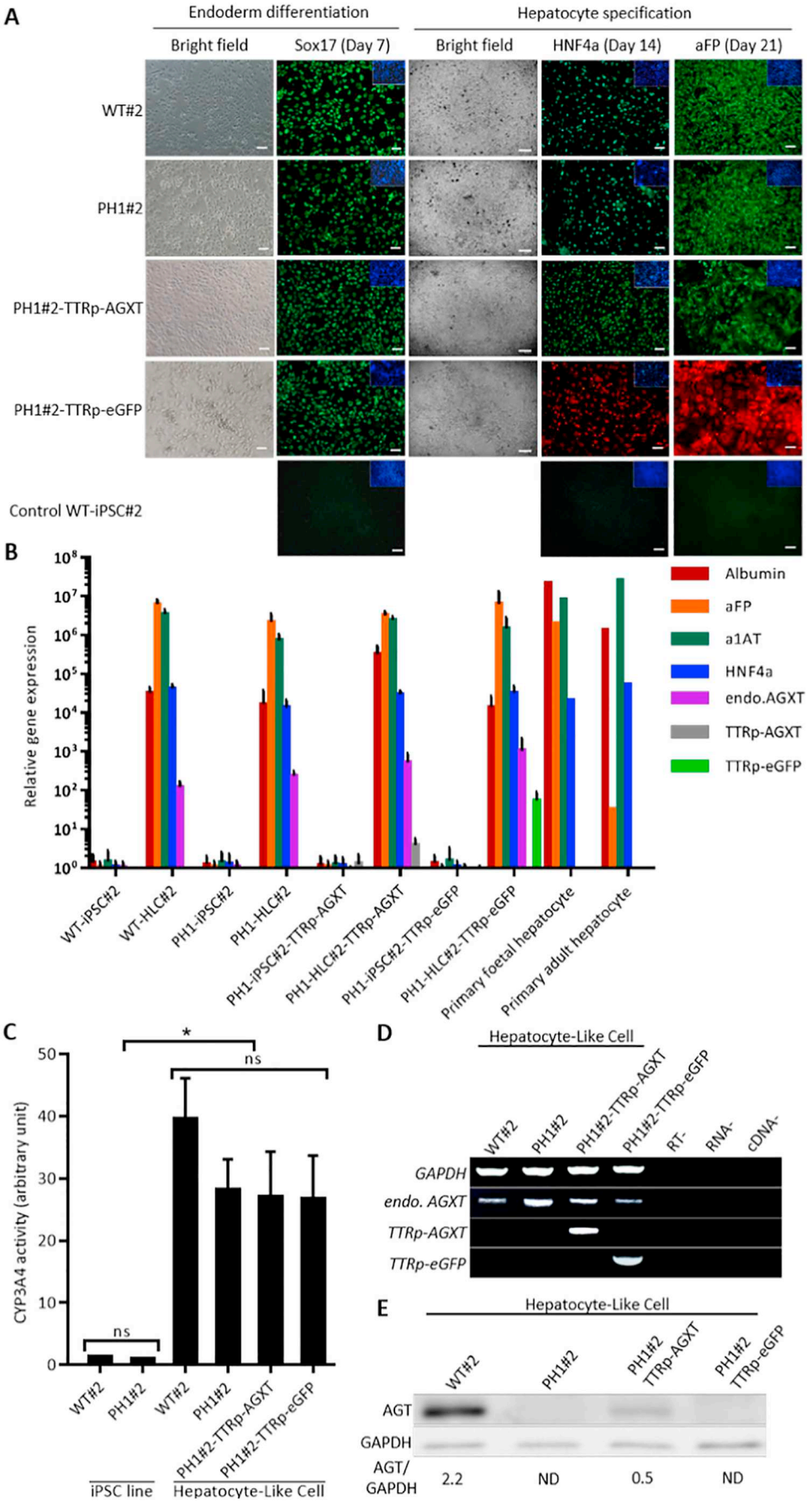

Fig. 5. Characterization of hepatocyte-like cells (HLCs) and analysis of AGT expression rescue.

(A) Bright field and immunofluorescence staining of endodermic (SOX17) and hepatic markers (HNF4a and aFP) throughout hepatocyte differentiation. Nuclei were localized by DAPI (blue). Scale bars, 100 µm. Magnification, 100X. (B) RT-qPCR analysis of hepatic gene markers in HLCs at day 31 of hepatocyte differentiation. Gene expression was normalized to the endogenous *HuP0* gene and data are means ± SD of four independent experiments. (C) CYP3A4 activity analysis in HLCs at day 31 of differentiation. Data were expressed as means ± SD of three independent experiments; *, $p < 0.05$. (D) RT-PCR analysis of eGFP and endogenous (endo. AGXT) or exogenous AGXT expression in HLCs. (E) Western blotting analysis of AGT protein expression in HLCs. ND; not determined. Abbreviations: aFP, alpha-fetoprotein; a1AT, alpha-1 antitrypsin; ns, non-significant; endo., endogenous. (For interpretation of the references to colour in this figure legend, the reader is referred to the web version of this article.)

protein levels in differentiated hepatocyte-like cells. Furthermore, we demonstrated the neutral effect of genome modification on the hepatic differentiation process. However, caution is required regarding the exhaustive consequences of genomic lentiviral integration. Despite numerous safety improvements in lentiviral vectors (Cavazzana-Calvo and Fischer, 2007), integration targeting is still challenging and insertional mutagenesis cannot be strictly ruled out unless fully investigated. For these reasons, strategies involving controlled genome modification would be beneficial for establishing safer gene therapy protocols. Recent advances in the field of targeted gene editing, mainly including CRISPR/Cas9 system (Fineran and Charpentier, 2012; Jinek et al., 2012), are likely to offer solutions. The efficacy of the targeted CRISPR/Cas9 DNA break in enhancing therapeutic homology-directed repair has been demonstrated in numerous studies, including hepatic diseases, and could be a powerful alternative to viral vectors for PH1 gene therapy (Lee et al., 2016; Pankowicz et al., 2017). However, we recently demonstrated that homology-directed repair is rare compared with NHEJ pathway leading to on-target indels and unexpected chromosomal truncations resulting from only one Cas9 nuclease-induced DSB by a p53-dependent mechanism (Cullot et al., 2019). Base editing is a newer genome-editing approach combining CRISPR systems together with DNA modificating enzymes to directly introduce point mutations into cellular DNA (Gaudelli et al., 2017). In recent studies, the authors were able to efficiently convert targeted G·C base pairs to A·T without DNA cleavage with high efficiency in human cells (Nishimasu et al., 2018). This strategy would be applied to reverse the c.731 T > C mutation of the *AGXT* gene responsible for hyperoxaluria in our PH1 patient.

5. Conclusion and/or summary

Human induced pluripotent stem cells can differentiate into hepatocyte like-cells with the potential of clinical and experimental use for inherited liver diseases. We generated PH1-iPSCs free of reprogramming factors from a patient with primary hyperoxaluria type 1 and demonstrated efficient hepatic lineage differentiation *in vitro*. In a gene therapy experiment, we rescued AGT expression in hepatocyte-like cells from PH1-iPSCs transduced with a therapeutic liver-specific lentiviral vector. Taken together, our results pave the way for studying and correcting primary hyperoxaluria type 1 using hepatocyte-like cells derived from patient-specific induced pluripotent stem cells.

Authors' contributions

E.R.: conception and design, data analysis and interpretation, manuscript writing; J.E. and J.M.B.: collection and/or assembly of data, data analysis and interpretation, manuscript writing; A.Be. and F.M.G.: data analysis and interpretation; J.H. and B.L: provision of study material or patients; A.Bi., M.L., I.M., L.A.M and P.D.: collection and/or assembly of data. All authors: final approval of manuscript.

Disclosure of potential conflicts of interest

The authors indicate no potential conflicts of interest.

Acknowledgments

This work was supported by research grants from Association Française contre les Myopathies (AFM), Fondation du rein, Association pour l'Information et la Recherche sur les maladies Rénales Génétiques (AIRG France), Oxalosis and Hyperoxaluria Foundation (OHF), Institut National de la Santé et de la Recherche Médicale (INSERM), Université de Bordeaux. We thank Dr. D. Trono and Dr. TH. Nguyen for the mTTR promoter, Dr. C. Grosset for liver cell mRNA, Dr. E. Salido for the modified human AGXT cDNA, and Dr. C. Danpure and Dr. S. Fargue for the AGT antibodies.

Appendix A. Supplementary data

Supplementary data to this article can be found online at https://doi.org/10.1016/j.scr.2019.101467.

References

Alonso, M.H., Ryckman, F.C., 1998. Current concepts in pediatric liver transplant. Semin. Liver Dis. 18, 295–307.
Annoni, A., Cantore, A., Della Valle, P., Goudy, K., Akbarpour, M., Russo, F., Bartolaccini, S., D'Angelo, A., Roncarolo, M.G., Naldini, L., 2013. Liver gene therapy by lentiviral vectors reverses anti-factor IX pre-existing immunity in haemophilic mice. EMBO Mol. Med. 5, 1684–1697.
Asplund, A., Pradip, A., Giezen, M. van, Aspegren, A., Choukair, H., Rehnström, M., Jacobsson, S., Ghosheh, N., Hajjam, D.E., Holmgren, S., Larsson, S., Benecke, J., Butron, M., Wigander, A., Noaksson, K., Sartipy, P., Björquist, P., Edsbagge, J., Küppers-Munther, B., 2016. One standardized differentiation procedure robustly generates homogenous hepatocyte cultures displaying metabolic diversity from a large panel of human pluripotent stem cells. Stem Cell Rev. Rep. 12, 90–104.
Ban, H., Nishishita, N., Fusaki, N., Tabata, T., Saeki, K., Shikamura, M., Takada, N., Inoue, M., Hasegawa, M., Kawamata, S., Nishikawa, S.-I., 2011. Efficient generation of transgene-free human induced pluripotent stem cells (iPSCs) by temperature-sensitive Sendai virus vectors. Proc. Natl. Acad. Sci. U. S. A. 108, 14234–14239.
Baxter, M., Withey, S., Harrison, S., Segeritz, C.-P., Zhang, F., Atkinson-Dell, R., Rowe, C., Gerrard, D.T., Sison-Young, R., Jenkins, R., Henry, J., Berry, A.A., Mohamet, L., Best, M., Fenwick, S.W., Malik, H., Kitteringham, N.R., Goldring, C.E., Piper Hanley, K., Vallier, L., Hanley, N.A., 2015. Phenotypic and functional analyses show stem cell-derived hepatocyte-like cells better mimic fetal rather than adult hepatocytes. J. Hepatol. 62, 581–589.
Beck, B.B., Habbig, S., Dittrich, K., Stippel, D., Kaul, I., Koerber, F., Goebel, H., Salido, E.C., Kemper, M., Meyburg, J., Hoppe, B., 2012. Liver cell transplantation in severe infantile oxalosis—a potential bridging procedure to orthotopic liver transplantation? Nephrol. Dial. Transplant. 27, 2984–2989.
Bedel, A., Taillepierre, M., Guyonnet-Duperat, V., Lippert, E., Dubus, P., Dabernat, S., Mautuit, T., Cardinaud, B., Pain, C., Rousseau, B., Lalanne, M., Ged, C., Duchartre, Y., Richard, E., de Verneuil, H., Moreau-Gaudry, F., 2012. Metabolic correction of congenital erythropoietic porphyria with iPSCs free of reprogramming factors. Am. J. Hum. Genet. 91, 109–121.
Bergstralh, E.J., Monico, C.G., Lieske, J.C., Herges, R.M., Langman, C.B., Hoppe, B., Milliner, D.S., 2010. Transplantation outcomes in primary hyperoxaluria. Am. J. Transplant. 10, 2493–2501.
Cantore, A., Ranzani, M., Bartholomae, C.C., Volpin, M., Della Valle, P., Sanvito, F., Sergi Sergi, L., Gallina, P., Benedicenti, F., Bellinger, D., Raymer, R., Merricks, E., Bellintani, F., Martin, S., Doglioni, C., D'Angelo, A., VandenDriessche, T., Chuah, M.K., Schmidt, M., Nichols, T., Montini, E., Naldini, L., 2015. Liver-directed lentiviral gene therapy in a dog model of hemophilia B. Sci. Transl. Med. 7 (277ra28).
Castello, R., Borzone, R., D'Aria, S., Annunziata, P., Piccolo, P., Brunetti-Pierri, N., 2016. Helper-dependent adenoviral vectors for liver-directed gene therapy of primary hyperoxaluria type 1. Gene Ther. 23, 129–134.
Cavazzana-Calvo, M., Fischer, A., 2007. Gene therapy for severe combined immunodeficiency: are we there yet? J. Clin. Invest. 117, 1456–1465.
Cochat, P., Fargue, S., Harambat, J., 2010. Primary hyperoxaluria type 1: strategy for organ transplantation. Curr. Opin. Organ Transpl. 15, 590–593.
Cochat, P., Hulton, S.-A., Acquaviva, C., Danpure, C.J., Daudon, M., De Marchi, M., Fargue, S., Groothoff, J., Harambat, J., Hoppe, B., Jamieson, N.V., Kemper, M.J., Mandrile, G., Marangella, M., Picca, S., Rumsby, G., Salido, E., Straub, M., van Woerden, C.S., 2012. Primary hyperoxaluria Type 1: indications for screening and guidance for diagnosis and treatment. Nephrol. Dial. Transplant. 27, 1729–1736.
Cullot, G., Boutin, J., Toutain, J., Prat, F., Pennamen, P., Rooryck, C., Teichmann, M., Rousseau, E., Lamrissi-Garcia, I., Guyonnet-Duperat, V., Bibeyran, A., Lalanne, M., Prouzet-Mauléon, V., Turcq, B., Ged, C., Blouin, J.M., Richard, E., Dabernat, S., Moreau-Gaudry, F., Bedel, A., 2019. CRISPR-Cas9 genome editing induces megabase-scale chromosomal truncations. Nat. Commun. 10, 1136.
Dindo, M., Oppici, E., Dell'Orco, D., Montone, R., Cellini, B., 2018. Correlation between the molecular effects of mutations at the dimer interface of alanine–glyoxylate aminotransferase leading to primary hyperoxaluria type I and the cellular response to vitamin B6. J. Inherit. Metab. Dis. 41, 263–275.
Fineran, P.C., Charpentier, E., 2012. Memory of viral infections by CRISPR-Cas adaptive immune systems: acquisition of new information. Virology 434, 202–209.
Fukuda, T., Takayama, K., Hirata, M., Liu, Y.-J., Yanagihara, K., Suga, M., Mizuguchi, H., Furue, M.K., 2017. Isolation and expansion of human pluripotent stem cell-derived hepatic progenitor cells by growth factor defined serum-free culture conditions. Exp. Cell Res. 352, 333–345.
Gao, X., Liu, Y., 2017. A transcriptomic study suggesting human iPSC-derived hepatocytes potentially offer a better in vitro model of hepatotoxicity than most hepatoma cell lines. Cell Biol. Toxicol. 33, 407–421.
Gaudelli, N.M., Komor, A.C., Rees, H.A., Packer, M.S., Badran, A.H., Bryson, D.I., Liu, D.R., 2017. Programmable base editing of a•T to G•C in genomic DNA without DNA cleavage. Nature 551, 464–471.
Ghosheh, N., Olsson, B., Edsbagge, J., Küppers-Munther, B., Van Giezen, M., Asplund, A., Andersson, T.B., Björquist, P., Carén, H., Simonsson, S., Sartipy, P., Synnergren, J., 2016. Highly synchronized expression of lineage-specific genes during in vitro hepatic differentiation of human pluripotent stem cell lines. Stem Cells Int. 2016.
Guengerich, F.P., 1999. CYTOCHROME P-450 3A4: regulation and role in drug

metabolism. Annu. Rev. Pharmacol. Toxicol. 39, 1–17.
Hannan, N.R., Segeritz, C.-P., Touboul, T., Vallier, L., 2013. Production of hepatocyte like cells from human pluripotent stem cells. Nat. Protoc. 8, 430–437.
Harambat, J., Fargue, S., Acquaviva, C., Gagnadoux, M.-F., Janssen, F., Liutkus, A., Mourani, C., Macher, M.-A., Abramowicz, D., Legendre, C., Durrbach, A., Tsimaratos, M., Nivet, H., Girardin, E., Schott, A.-M., Rolland, M.-O., Cochat, P., 2010. Genotype–phenotype correlation in primary hyperoxaluria type 1: the p.Gly170Arg AGXT mutation is associated with a better outcome. Kidney Int. 77, 443–449.
Harambat, J., Fargue, S., Bacchetta, J., Acquaviva, C., Cochat, P., 2011. Primary Hyperoxaluria. Int. J. Nephrol. 2011.
Hoppe, B., Beck, B.B., Milliner, D., 2009. The primary hyperoxalurias. Kidney Int. 75, 1264–1271.
Jiang, J., Salido, E.C., Guha, C., Wang, X., Moitra, R., Liu, L., Roy-chowdhury, J., Roy-chowdhury, N., 2008. Correction of hyperoxaluria by liver repopulation with hepatocytes in a mouse model of primary hyperoxaluria Type-1. Transplantation 85, 1253–1260.
Jinek, M., Chylinski, K., Fonfara, I., Hauer, M., Doudna, J.A., Charpentier, E., 2012. A programmable dual-RNA–guided DNA endonuclease in adaptive bacterial immunity. Science 337, 816–821.
Laurent, V., Fraix, A., Montier, T., Cammas-Marion, S., Ribault, C., Benvegnu, T., Jaffres, P.-A., Loyer, P., 2010. Highly efficient gene transfer into hepatocyte-like HepaRG cells: new means for drug metabolism and toxicity studies. Biotechnol. J. 5, 314–320.
Lee, P.C., Truong, B., Vega-Crespo, A., Gilmore, W.B., Hermann, K., Angarita, S.A., Tang, J.K., Chang, K.M., Wininger, A.E., Lam, A.K., Schoenberg, B.E., Cederbaum, S.D., Pyle, A.D., Byrne, J.A., Lipshutz, G.S., 2016. Restoring ureagenesis in hepatocytes by CRISPR/Cas9-mediated genomic addition to arginase-deficient induced pluripotent stem cells. Mol. Ther. Nucleic Acids 5, e394.
Mesa-Torres, N., Yunta, C., Fabelo-Rosa, I., Gonzalez-Rubio, J.M., Sánchez-Ruiz, J.M., Salido, E., Albert, A., Pey, A.L., 2014. The consensus-based approach for gene/enzyme replacement therapies and crystallization strategies: the case of human alanine–glyoxylate aminotransferase. Biochem. J. 462, 453–463.
Moreau-Gaudry, F., Xia, P., Jiang, G., Perelman, N.P., Bauer, G., Ellis, J., Surinya, K.H., Mavilio, F., Shen, C.K., Malik, P., 2001. High-level erythroid-specific gene expression in primary human and murine hematopoietic cells with self-inactivating lentiviral vectors. Blood 98, 2664–2672.
Newstead, C.G., 1998. Assessment of risk of cancer after renal transplantation. Lancet 351, 610–611.
Nguyen, T.H., Bellodi-Privato, M., Aubert, D., Pichard, V., Myara, A., Trono, D., Ferry, N., 2005. Therapeutic lentivirus-mediated neonatal in vivo gene therapy in hyperbilirubinemic Gunn rats. Mol. Ther. 12, 852–859.
Nishimasu, H., Shi, X., Ishiguro, S., Gao, L., Hirano, S., Okazaki, S., Noda, T., Abudayyeh, O.O., Gootenberg, J.S., Mori, H., Oura, S., Holmes, B., Tanaka, M., Seki, M., Hirano, H., Aburatani, H., Ishitani, R., Ikawa, M., Yachie, N., Zhang, F., Nureki, O., 2018. Engineered CRISPR-Cas9 nuclease with expanded targeting space. Science 361, 1259–1262.
Ohmori, T., Mizukami, H., Katakai, Y., Kawai, S., Nakamura, H., Inoue, M., Shu, T., Sugimoto, H., Sakata, Y., 2018. Safety of intra-articular transplantation of lentivirally transduced mesenchymal stromal cells for haemophilic arthropathy in a non-human primate. Int. J. Hematol. 1–7.
Okita, K., Yamanaka, S., 2011. Induced pluripotent stem cells: opportunities and challenges. Philos. Trans. R. Soc. Lond. Ser. B Biol. Sci. 366, 2198–2207.
Pankowicz, F.P., Jarrett, K.E., Lagor, W.R., Bissig, K.-D., 2017. CRISPR/Cas9: at the cutting edge of hepatology. Gut 66, 1329–1340.
Rashid, S.T., Corbineau, S., Hannan, N., Marciniak, S.J., Miranda, E., Alexander, G., Huang-Doran, I., Griffin, J., Ahrlund-Richter, L., Skepper, J., Semple, R., Weber, A., Lomas, D.A., Vallier, L., 2010. Modeling inherited metabolic disorders of the liver using human induced pluripotent stem cells. J. Clin. Invest. 120, 3127–3136.
Richard, E., Robert, E., Cario-André, M., Ged, C., Géronimi, F., Gerson, S.L., Verneuil, H. de, Moreau-Gaudry, F., 2004. Hematopoietic stem cell gene therapy of murine protoporphyria by methylguanine-DNA-methyltransferase-mediated *in vivo* drug selection. Gene Ther. 11, 1638–1647.
Roy-Chowdhury, N., Wang, X., Guha, C., Roy-Chowdhury, J., 2017. Hepatocyte-like cells derived from induced pluripotent stem cells. Hepatol. Int. 11, 54–69.
Salido, E.C., Li, X.M., Lu, Y., Wang, X., Santana, A., Roy-Chowdhury, N., Torres, A., Shapiro, L.J., Roy-Chowdhury, J., 2006. Alanine–glyoxylate aminotransferase-deficient mice, a model for primary hyperoxaluria that responds to adenoviral gene transfer. Proc. Natl. Acad. Sci. U. S. A. 103, 18249–18254.
Salido, E., Rodriguez-Pena, M., Santana, A., Beattie, S.G., Petry, H., Torres, A., 2011. Phenotypic correction of a mouse model for primary hyperoxaluria with adeno-associated virus gene transfer. Mol. Ther. 19, 870–875.
Santana, A., Salido, E., Torres, A., Shapiro, L.J., 2003. Primary hyperoxaluria type 1 in the Canary Islands: a conformational disease due to I244T mutation in the P11L-containing alanine:glyoxylate aminotransferase. Proc. Natl. Acad. Sci. U. S. A. 100, 7277–7282.
Schmitt, F., Remy, S., Dariel, A., Flageul, M., Pichard, V., Boni, S., Usal, C., Myara, A., Laplanche, S., Anegon, I., Labrune, P., Podevin, G., Ferry, N., Nguyen, T.H., 2010. Lentiviral vectors that express UGT1A1 in liver and contain miR-142 target sequences normalize hyperbilirubinemia in Gunn rats. Gastroenterology 139, 999–1007.e2.
Takahashi, K., Tanabe, K., Ohnuki, M., Narita, M., Ichisaka, T., Tomoda, K., Yamanaka, S., 2007. Induction of pluripotent stem cells from adult human fibroblasts by defined factors. Cell 131, 861–872.
Takayama, K., Hagihara, Y., Toba, Y., Sekiguchi, K., Sakurai, F., Mizuguchi, H., 2018. Enrichment of high-functioning human iPS cell-derived hepatocyte-like cells for pharmaceutical research. Biomaterials 161, 24–32.
Trevisan, M., Desole, G., Costanzi, G., Lavezzo, E., Palù, G., Barzon, L., 2017. Reprogramming methods do not affect gene expression profile of human induced pluripotent stem cells. Int. J. Mol. Sci. 18.
Zapata-Linares, N., Rodriguez, S., Salido, E., Abizanda, G., Iglesias, E., Prosper, F., Gonzalez-Aseguinolaza, G., Rodriguez-Madoz, J.R., 2016. Generation and characterization of human iPSC lines derived from a primary Hyperoxaluria Type I patient with p.I244T mutation. Stem Cell Res. 16, 116–119.
Zhang, S., Chen, S., Li, W., Guo, X., Zhao, P., Xu, J., Chen, Y., Pan, Q., Liu, X., Zychlinski, D., Lu, H., Tortorella, M.D., Schambach, A., Wang, Y., Pei, D., Esteban, M.A., 2011. Rescue of ATP7B function in hepatocyte-like cells from Wilson's disease induced pluripotent stem cells using gene therapy or the chaperone drug curcumin. Hum. Mol. Genet. 20, 3176–3187.
Zufferey, R., Dull, T., Mandel, R.J., Bukovsky, A., Quiroz, D., Naldini, L., Trono, D., 1998. Self-inactivating lentivirus vector for safe and efficient in vivo gene delivery. J. Virol. 72, 9873–9880.